2021

Upgraded Algebraic Solution for Isobutane Flows in Diabatic Capillary Tubes

Luka Lorbek
University of Ljubljana, Slovenia, luka.lorbek@fs.uni-lj.si

Christian Hermes
Federal University of Santa Catarina

Joaquim Gonçalves
Federal University of Santa Catarina

Upgraded Algebraic Solution for Isobutane Flows in Diabatic Capillary Tubes

Luka LORBEK [1,*], Joaquim M. GONÇALVES [2], Christian J. L. HERMES [3]

[1] Laboratory for Refrigeration and District Energy, Faculty of Mechanical Engineering, University of Ljubljana
Ljubljana, Slovenia

[2] Refrigeration and Air Conditioning Unit, Federal Institute of Santa Catarina
São José, Santa Catarina, Brazil

[3] POLO Research Laboratories, Department of Mechanical Engineering, Federal University of Santa Catarina
Florianópolis, Santa Catarina, Brazil

[*] Corresponding Author, luka.lorbek@fs.uni-lj.si

ABSTRACT

The present work advances an algebraic model for predicting the suction line outlet temperature and the mass flow rate in diabatic capillary tube flows. The proposed solution improved the functionality of an existing model, without significantly increasing the complexity of its implementation. The approach introduced in this paper assumes the refrigerant flow in the capillary tube as adiabatic to describe the two-phase temperature profile. By doing so, the ordinary differential equation governing the energy conservation in the suction line can be solved analytically. The model predictions for the refrigerant mass flow rate and the temperature difference through the suction line were compared against 51 experimental data points, showing errors within 10% and 15% bounds, respectively. Nonetheless, it was observed that the experimental dataset was restricted to the cases where heat transfer takes place also in the single-phase region of the capillary tube. Therefore, model validation for cases where heat exchange takes place exclusively in the two-phase region is still to be performed.

1. INTRODUCTION

Capillary tubes have been used as expansion devices in small capacity refrigeration systems for nearly a century. In order to improve the specific refrigerating effect in the evaporator, avoid compressor slugging, and prevent suction line condensation, the capillary tube is put in thermal contact with the suction line forming a counter-flow heat exchanger. Modelling of the refrigerant flow in the so-called capillary tube suction line heat exchangers (CTSLHXs) has caught the attention of both researchers and engineers, who are interested in predicting complex compressible fluid flow with phase-change and heat transfer phenomena (Escanes *et al*., 1994; Chen *et al*., 2005; Garcia-Valladares *et al*., 2007; Hermes *et al*. 2008; Seixlack *et al*., 2009; Ablanque *et al*., 2015).

CTSLHXs models are generally classified as either distributed or lumped. In the former, the capillary tubes are discretized into control volumes, so that the mass flow rate and the suction line outlet temperature are solved numerically. The latter rely on simplifying assumptions to reduce the problem to explicit algebraic equations for predicting the mass flow rate and the suction line outlet temperature. The main advantage of the lumped approach is its short computational time compared to the distributed one, which makes it suitable not only for "back-of-the-envelope" calculations but also for integration with high-level system simulation tools. However, such an approach relies on empirical coefficients to compensate for the assumptions required to simplify the mathematical formulation (Yilmaz and Umal, 1996; Zhang and Ding, 2004; Hermes *et al*., 2010a, 2010b), thus lacking generality.

In a previous work, Hermes *et al*. (2010b) assumed a balanced counter-flow heat exchanger (i.e., parallel temperature profiles) to describe the heat transfer between the capillary tube and the suction line. An empirical $-\pi$type correlation was used to correct the refrigerant mass flow rate, computed beforehand from a lumped model considering the flow as adiabatic (Hermes *et al*. 2010a). However, the assumption may be inaccurate when the heat exchanger is positioned closer to the capillary tube exit region, where two-phase refrigerant is expanding at higher rates (see Fig. 1). In addition, recent studies of modern refrigerators operating with isobutane have shown that, in several applications, vapor is drawn into the capillary tube inlet (Boeng and Melo, 2012; Lee *et al*., 2016; Martinez-Ballester *et al*., 2017). In such cases, the entire CTSLHX is located in the two-phase region of the capillary tube. Therefore, the present paper is aimed at expanding the capabilities of the model proposed by Hermes *et al*. (2010b) using an improved analytical solution for calculating the heat transfer between the suction line and the two-phase refrigerant in the capillary tube.

2. MATHEMATICAL MODELING

2.1 Heat Transfer in the Two-Phase Region

In general, the suction line is placed in contact with the single-phase region of the capillary tube, where the heat transfer effectiveness is higher, as the temperature in the two-phase region rapidly decreases due to refrigerant expansion. However, the suction line can sometimes extend into the two-phase region of the capillary tube because of manufacturing constraints. In such cases, the temperature profiles are similar to those depicted in Figure 1.

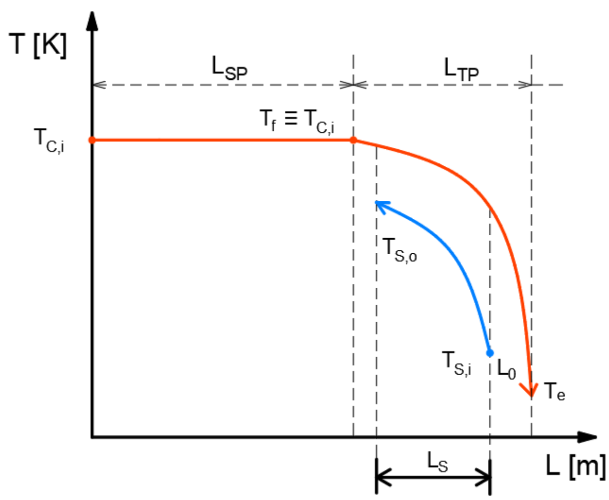

Figure 1: Temperature profiles of the CTSLHX in the case where the suction line is located entirely in the two-phase region.

The energy conservation for an infinitesimal volume of the suction line can be expressed as follows:

$$\dot{m}c_{p,S}dT_S = UdA(T_C - T_S) \tag{1}$$

where $\dot{m}$ is the mass flow rate, $c_{p,S}$ is the specific heat of vapor in the suction line, dT_S is the infinitesimal temperature increment of the suction line, U is the overall heat transfer coefficient evaluated locally, and T_C and T_S are the capillary tube and suction line temperatures, respectively. Assuming a constant cross section, the heat transfer area dA can be expressed as $dA = P(-dL)$, where dL is the infinitesimal length of the volume, and $P = \pi D_S$ is the perimeter of the tube. Rearranging Equation (1) yields the following ordinary differential equation for the suction line temperature,

$$\frac{dT_S}{dL} = m(T_S - T_C) \tag{2}$$

where $m = UP/\dot{m}c_{p,S}$, assumed constant for the entire CTSLHX. For the sake of simplicity, a dimensionless length $\zeta = L/L_{tp}$ was adopted, where 0 is the location of the flashing point and 1 is the capillary tube outlet. Equation (2) is subjected to the following boundary condition, $T_S(\zeta = \zeta_0) = T_{S,i}$, where $\zeta_0 = L_0/L_{tp}$ is the position of the suction line inlet taking the capillary tube outlet as the referential.

In order to obtain an explicit solution for Equation (2), an expression for the capillary tube temperature profile, T_C, is needed. It should be noted that the temperature profile in the capillary tube two-phase region is governed by the pressure drop and the heat transfer. The effect of the pressure drop is straightforward, as the saturation temperature is set by the vapor pressure. The heat transfer, on the other hand, plays an indirect role, as it reduces the vapor quality along the heat exchanger length, thus increasing the mass flux and, therefore, the pressure drop. In this work, it has been hypothesized that the effect of heat transfer is overruled by the pressure drop, so that the temperature profile in the two-phase region is independent of whether the capillary tube is adiabatic or not. Following the assumption of adiabatic flow, Yilmaz and Unal (1996) proposed the following expression for the length of the two-phase region in capillary tubes,

$$L_{tp} = \frac{2D_C}{f_{tp}G^2}\left[\frac{p_f - p_e}{a} + \frac{b}{a^2}\ln\left(\frac{ap_e + b}{ap_f + b}\right) - G^2\ln\left(\frac{v_e}{v_f}\right)\right] \tag{3}$$

where $a = v_f(1-k)$, $b = v_f p_f k$ and $k = 1.63 \cdot 10^5 p_f^{0.72}$ (Zhang and Ding 2004). In addition to returning the two-phase length, Equation (3) can also provide intermediate lengths L by replacing p_e by the saturated pressure p_{sat} calculated from the Antoine equation, as follows:

$$log(p_{sat}) = A - \frac{B}{T_C + C} \tag{4}$$

where, for isobutane, $A = 4.00272$, $B = 947.54$, $C = 248.87$ (Poling, 2001), with the pressure in [bar] and the temperature in [°C]. Combining Equation (3) and Equation (4) yields an expression for the temperature profile in the capillary tube as a function of the two-phase length from the flash point, $T_C(\zeta)$, which can be inserted into Equation (2) to obtain $T_S(\zeta)$. However, since the temperature cannot be expressed explicitly, integration of Equation (2) cannot be performed analytically. An alternative solution was found by fitting a dimensionless capillary tube temperature as a function of ζ, as follows:

$$\theta(\zeta) = \frac{T_C(\zeta) - T_e}{T_f - T_e} = \theta_0 + \theta_1\zeta + \theta_2\zeta^2 + \theta_3\zeta^3 + \theta_4\zeta^4 \tag{5}$$

where θ is the dimensionless capillary tube temperature, $\theta_0 = 1.06 - 8.87 \cdot 10^{-5}G + 2.60 \cdot 10^{-8}G^2$, $\theta_1 = 0.0195$, $\theta_2 = -1.04$, $\theta_3 = 2.08$, $\theta_4 = -1.65$, $G = (4\dot{m}/\pi D_C^2)$ is the refrigerant mass flux, T_f is the temperature of the flash-point, and T_e is determined from the saturation temperature corresponding to the pressure at the capillary exit, $p_e = max|p_{evap}, p_{sonic}|$, where $p_{sonic} = G\sqrt{b}$. Figure 2 shows several temperature profiles for different flashing temperatures and mass fluxes, according to Equation (3), along with the corresponding temperature profiles obtained from the polynomial fit (Equation 5).

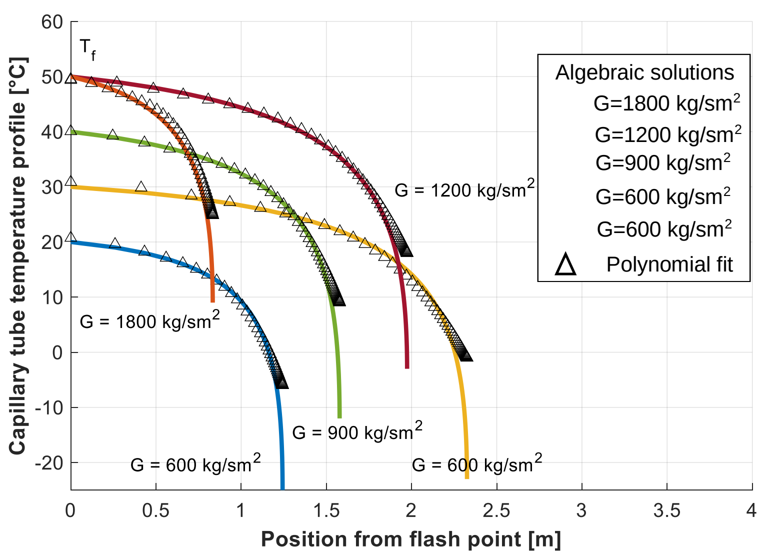

Figure 2: Capillary tube temperature profiles in the two-phase region and corresponding polynomial fits.

Due to the large gradients towards the capillary tube outlet, the proposed polynomial fit worsens significantly if fitted on the whole domain. To overcome this, the polynomial was only fitted using the first 80% of the two-phase temperature profile. This means that the solution will not be accurate if the suction line is extended to the very end of the capillary tube – a situation not likely to take place in practice. Regardless, the capillary tube temperature profile obtained from Equation (5) is used only for integrating Equation (2), yielding

$$T_S(\zeta) = T_{S,i}e^{n(\zeta-\zeta_0)} + n^{-4}\left[(\alpha+\beta)\left(1-e^{n(\zeta-\zeta_0)}\right)\right] \tag{6}$$

where $n = mL_{tp}$, and α and β are the following functions of n and ζ:

$$\alpha = \alpha_0 n^4 + \alpha_1 n^3 + 2\alpha_2 n^2 + 6\alpha_3 n + 24\alpha_4 \tag{7}$$

$$\begin{aligned}\beta = (\alpha_1 n^4 + 2\alpha_2 n^3 + 6\alpha_3 n^2 + 24\alpha_4 n)\zeta + (\alpha_2 n^4 + 3\alpha_3 n^2 + 12\alpha_4 n^2)\zeta^2 \\ + (\alpha_3 n^4 + 4\alpha_4 n^3)\zeta^3 + (\alpha_4 n^4)\zeta^4\end{aligned} \tag{8}$$

where $\alpha_0 = T_e + \theta_0(T_f - T_e)$ and $\alpha_{1\ldots4} = \theta_{1\ldots4}(T_f - T_e)$.

2.2 Heat Transfer in the Single-Phase Region

Figure 3 shows the temperature profiles of the capillary tube and suction line for single-phase only (b), and combined single/two-phase heat transfer (a). In such cases, the effectiveness method was adopted to calculate the heat transfer rate in the single-phase region, so that

$$\dot{Q} = C_c(T_{C,i} - T_f) = C_s(T_{S,o} - T_{S,i}) = \varepsilon C_{min}(T_{C,in} - T_{S,i}) \tag{9}$$

where

$$\varepsilon = \frac{1 - e^{-\frac{UA}{C_{min}}(1-C_r)}}{1 - C_r e^{-\frac{UA}{C_{min}}(1-C_r)}} \tag{10}$$

and $C_r = C_{min}/C_{max}$. In the case of combined single/two-phase heat transfer, $T_{S,in}$ in Equation (9) is considered to be the temperature of the suction line at the flashing point $T_{S,f}$.

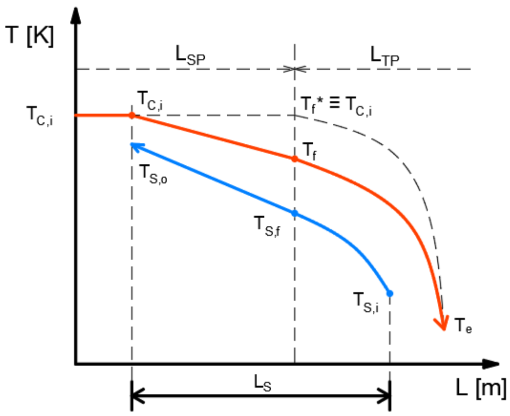

(a)

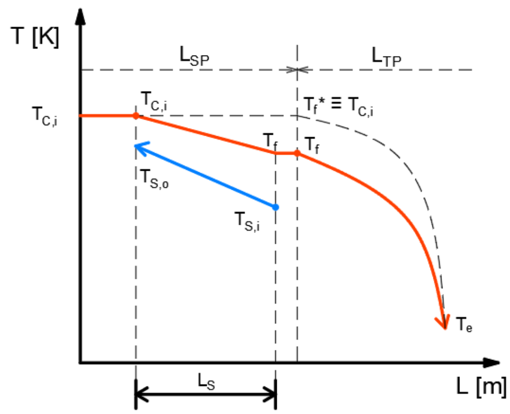

(b)

Figure 3: (a) the suction line heat exchanger is located in both the single- and two-phase region, and (b) the suction line heat exchanger is located entirely in the single-phase region.

2.3 Refrigerant Mass Flow Rate

The mass flow rate $\dot{m}$ through the capillary tube is determined from the following expression (introduced by Hermes *et al*., 2010a), considering the capillary tube flow as adiabatic:

$$\dot{m} = \phi \sqrt{\frac{D_C^5}{L_C}\left[\frac{p_i - p_f}{v_f} + \frac{p_f - p_e}{a} + \frac{b}{a^2}\ln\left(\frac{ap_e + b}{ap_f + b}\right)\right]} \tag{11}$$

where $\phi = 6$ and is associated with the friction factor (see Hermes *et al.*, 2010b). Additionally, an empirical π–type diabatic multiplier λ is adopted to account for the changes in the fluid dynamics caused by heat transfer (Hermes *et al*., 2010b), as follows:

$$\lambda = \frac{\dot{m}}{\dot{m}_{Eq.(11)}} = c_0 \left(\frac{L_S}{L_C}\right)^{c_1} \left(\frac{D_S}{D_C}\right)^{c_2} \varepsilon^{c_3} \left(\frac{v_f \mu_f}{v_e \mu_e}\right)^{c_3} \tag{12}$$

where $c_0 = 1.1031$, $c = 0.1897$, $c_2 = -0.3525$, $c = -0.3630$, and $c_4 = -0.2603$ for concentric arrangements, and $c_0 = 1.1126$, $c_1 = 0.1813$, $c_2 = -0.3282$, $c_3 = -0.3667$, and $c_4 = -0.2869$ for lateral arrangements. The coefficients in Equation (12) were obtained by fitting the results to experimental data of Boeng *et al*. (2020) and Hermes *et al*. (2010b). The thermodynamic properties are determined at the flashing point and at the capillary tube exit conditions. The enthalpy at the capillary tube outlet was calculated from

$$h_{C,o} = h_{C,i} - \varepsilon c_{p,S}\left(T_{C,i} - T_{S,i}\right) \tag{13}$$

2.4 Closing Equations

The friction factors are obtained from Churchill's correlation (1977). The two-phase viscosity required to calculate the Reynolds number is determined as follows (Hermes *et al*., 2010a):

$$\frac{\mu_{tp}}{\mu_f} = \frac{8}{7}\left[\frac{1 - \left(p_e/p_f\right)^{7/8}}{1 - p_e/p_f}\right] \tag{14}$$

The thermal resistance between the capillary tube and suction line is assumed to be governed only by the convective heat transfer resistance in the suction line (Hermes *et al*., 2010b), as follows:

$$\frac{1}{UA} \approx \frac{1}{h_S A \eta_{fin}} \tag{15}$$

where U is the overall heat transfer coefficient, $A = \pi D_S L_s$ is the heat transfer area, h_s is the heat transfer coefficient in the suction line, and η_{fin} is the fin efficiency calculated from:

$$\eta_{fin} = \frac{\tanh\left(\psi L_{fin}\right)}{\psi L_{fin}} \tag{16}$$

where $\psi = \sqrt{2h_S/k_{Cu}t_S}$ and $L_{fin} = (\pi D_S + t_S)/2$. The suction line heat transfer coefficient is determined from:

$$h_S = \frac{k_S}{D}\left(Re_S^{\omega} Pr_S^{1/3}\right) \tag{17}$$

which has been calibrated to experimental data points from Boeng *et al*. (2020) and Hermes *et al*. (2010b) so that $\omega = 0.360$ for concentric, and $\omega = 0.405$ for lateral arrangements. The characteristic length, D, is the suction line inner diameter for lateral arrangements, and the capillary tube outer diameter for concentric arrangements. All thermodynamic properties are determined from the Coolprop library (Bell *et al*., 2014).

3. SOLUTION SCHEME

In the case of a heat transfer between the capillary tube and suction line located entirely in the two-phase region, an analytical solution can be obtained if the flow is not choked. Otherwise, an iterative procedure is required, as Equation (11) becomes implicit. In the case of a combined single- and two-phase heat transfer in the CTSLHX, the equation set cannot be solved explicitly, and an iterative procedure is required regardless of whether the flow is choked or not. For all three cases the solution algorithm starts by assuming that $T_f = T_{C,i}$, and then proceeds to:

1) calculate the mass flow rate from Eq. (11);
2) determine if the capillary tube flow is choked;
3) determine the two-phase length from Eq. (3) and the single-phase length from $L_{sp} = L_C - L_{tp}$;
4) evaluate the outlet enthalpy, the transport properties of the suction line and capillary tube, and two-phase friction factor in the capillary tube;

Based on the position of the flashing point with respect to the suction line, the algorithm then decides whether the case is single- (Fig. 3b) or two-phase only (Fig. 1), or a combination both (Fig. 3a). It then proceeds to determine:

5) the overall heat transfer coefficient (U) and the number of transfer units (n);
6) the suction line temperature at the position where flashing occurs in the capillary tube:
   for a combined case $T_{S,f} = T_{S,Eq.(6)}(\zeta = 0)$ (see Fig. 3a);
   for a single-phase only case $T_{S,f} = T_{S,i}$ (see Fig 3b);
7) Next, the suction line outlet temperature is obtained from $T_{S,o} = \varepsilon C_{min}(T_{C,in} - T_{S,f})/C_s + T_{S,f}$; (in case of a two-phase only solution, the suction line outlet temperature is obtained directly from Equation 6).
8) A new estimate of the flashing temperature is then obtained from $T_f = T_{C,in} - C_S(T_{S,o} - T_{S,f})/C_C$; (this step is skipped if the solution is two-phase only)
9) If the change in the mass flow rate and flashing temperature is lower than the tolerance level, the algorithm stops. Otherwise, returns to step 1.

4. RESULTS

Figure 4 shows a solution of the capillary tube suction line heat exchange for an arbitrary test case running with R600a, where the suction line is located entirely in the two-phase region of the capillary tube. The results are plotted for different values of the number of transfer units n considering a flashing temperature of 40 °C, a mass flow rate of 1.8 kg/h, and a suction line inlet temperature of 3.4°C. The internal capillary tube and suction line diameters are 0.75 mm and 6.0 mm, respectively, and the two-phase length is equal to 1.07 m. One can see that the polynomial fit (Equation 5) accurately describes the adiabatic capillary tube temperature profile in the region where heat exchange with the suction line is taking place. This shows that limiting the polynomial fit to the first 80% of the two-phase region does not compromise the solution, unless the suction line is extended towards the very end of the capillary tube.

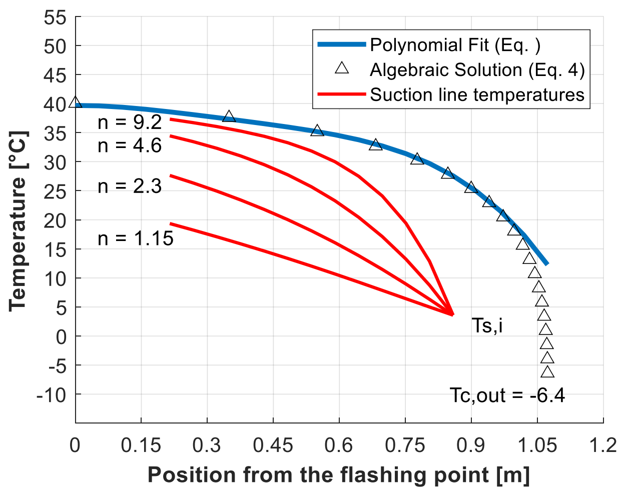

Figure 4: Capillary tube and suction line temperature profiles for different values of *n*

Similarly, Figure 5 shows the profiles in the case of a combined single/two-phase heat exchange. In the two-phase region, the suction line temperature profile is calculated from Equation (6), whereas in the single-phase region Equation (9) is adopted. It is evident that the model can now distinguish between situations where the capillary tube and suction line temperature profiles can be assumed as parallel, and situations where it is necessary to consider the temperature profiles as non-linear. The model was then compared against 51 measured mass flow rates and suction line temperature differences (outlet minus inlet) using isobutane (R-600a) as the refrigerant. The measurements were obtained from Boeng *et al*. (2020) and Hermes *et al*. (2010b). Both lateral and concentric CTSLHX arrangements were compared, although it should be noted that the concentric arrangements are no longer used in modern refrigerators. The model was able to determine 82% of all mass flow rates (see Figure 6) and 84% of all suction line temperature differences (see Figure 7) within a ±10% error band. Similarly, it determined 88% of all mass flow rates, and 98% of all suction line temperature differences within ±15% error bounds. However, none of the experimental points returned an entirely two-phase heat transfer scenario.

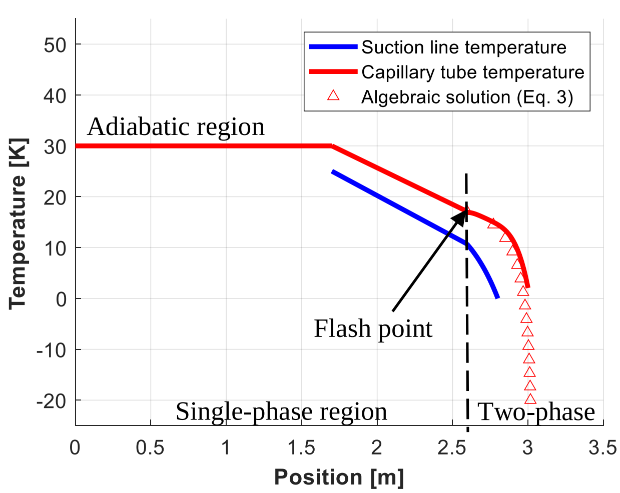

Figure 5: Capillary tube and suction line temperature profiles for a combined single/two-phase heat exchange case.

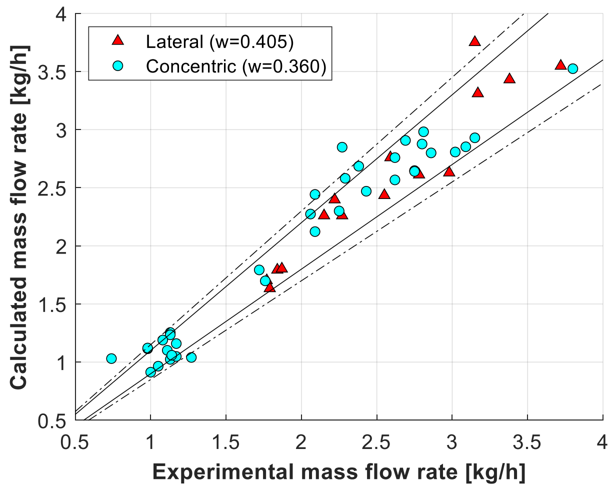

Figure 6: Calculated vs. experimental mass flow rates in a ±10% and ±15% error margin.

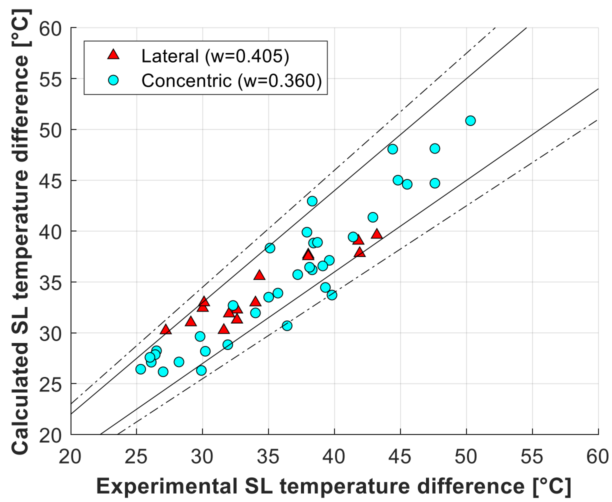

Figure 7: Calculated vs. experimental suction line temperature differences in a ±10% and ±15% error margin.

5. CONCLUSIONS

Simplified CTSLHX models require new approaches for calculating the heat transfer in the two-phase region of the capillary tube. Therefore, the model presented by Hermes *et al*. (2010b) was upgraded with an analytical solution of the CTSLHX heat exchange in the two-phase region, thereby increasing the functionality without significantly penalizing the its complexity. By assuming that the two-phase refrigerant flow in the capillary tube behaves as adiabatic, despite heat transfer to the suction line, an expression for the capillary tube temperature profile could be obtained from a polynomial fit. This expression was then inserted into the differential equation describing the energy balance in the suction line, which was then integrated algebraically to obtain an algebraic solution of the suction line temperature profile. An iterative algorithm was implemented to couple this methodology with the effectiveness method for cases where heat transfer also takes place in the single-phase region. The model was compared to 51 experimental points using isobutane as the refrigerant, considering both concentric and lateral configurations. It was able to determine 82% to 88% of all mass flow rates, and 84% to 98% of all suction line inlet-outlet temperature differences within ±10% to ±15% error bounds, respectively. However, the experimental points constituted cases where heat transfer occurred also in the single-phase area. Therefore, additional experimental points where heat transfer takes place exclusively in the two-phase region are required to fully validating the model.

NOMENCLATURE

A	surface/area	(m^2)
C	capacity	(W/K)
c_p	specific heat	(J/kgK)
D	diameter	(m)
f	Darcy's friction factor	(-)
G	mass flux	(kg/sm^2)
h	enthalpy/heat transfer coeff.	(J/kg) or (W/m^2K)
k	thermal conductivity	(W/mK)
L	length	(m)
$\dot{m}$	mass flow rate	(kg/s)
n	number of transfer units	(-)
P	perimeter	(m)
p	pressure	(Pa)
Pr	Prandtl number	(-)
$\dot{Q}$	heat flow rate	(W)
Re	Reynolds number	(-)
t	fin (suction line) thickness	(m)
T	temperature	(K)
U	overall heat transfer coefficient	(W/m^2K)
v	specific volume	(m^3/kg)

Greek symbols

α, β	polynomial functions	(-)
ε	heat transfer effectiveness	(-)
ζ	relative length	(-)
η	fin efficiency	(-)
θ	dimensionless temperature	(-)
λ	diabatic multiplier	(-)
μ	dynamic viscosity	(Pas)

Subscripts

0	start/inlet
C	capillary tube
Cu	copper
e	evaporating
evap	evaporating
f	flashing
fin	fin
i	inner/in
max	maximal
min	minimal
o	outer/out
S	suction line
sat	saturated
sonic	sonic
sp	single-phase
tp	two-phase

REFERENCES

Ablanque, N., Oliet, C., Rigola, J. & Oliva, A. (2015). Numerical simulation of non-adiabatic capillary tubes. Special emphasis on the near-saturation zone. Int. J. Refrig., 55, 153–167.

Bell, I.H., Wronski, J., Quoilin, S. & Lemort, V. (2014). Pure and pseudo-pure fluid thermophysical property evaluation and the open-source thermophysical property library CoolProp. Ind. Eng. Chem. Res., 53, 2498–2508.

Boeng, J. & Melo, C. (2012). A capillary tube-refrigerant charge design methodology for household refrigerators – part II: Equivalent diameter and test procedure. Proc. Int. Refrig. Air Cond. Conf. at Purdue (2146–2156).

Boeng, J., Stahelin, R., Gonçalves, J.M. & Hermes, C.J.L. (2020) Performance ratings of concentric and lateral (taped, brazed and extruded) capillary tube suction line heat exchangers running with isobutane, Applied Thermal Engineering 171 (2020) 115079

Chen, Y. & Gu, J. (2005). Non-adiabatic capillary tube flow of carbon dioxide in a novel refrigeration cycle. Appl. Therm. Eng., 1670–1683.

Churchill, S. (1977). Friction-factor equation spans all fluid-flow regimes. Chem. Eng., 91–92.

Escanes, F., Perez-Segarra, C.D. & Oliva, A. (1995). Numerical simulation of capillary tube expansion devices. Int. J. Refrig., 18, 113–122.

Garcia-Valladares, O. (2007). Numerical simulation of non-adiabatic capillary tubes considering metastable region. Part I: Mathematical formulation and numerical model. Int. J. Refrig., 30, 642–653.

Hermes, C.J.L., Melo, C. & Gonçalves, J. (2008). Modeling of non-adiabatic capillary tube flows: a simplified approach and comprehensive experimental validation. Int. J. Refrig., 31, 1358–1367.

Hermes, C.J.L., Melo, C. & Knabben, F.T. (2010a). Explicit algebraic solution of capillary tube flows. Part I: adiabatic capillary tubes. Appl. Therm. Eng., 30, 449–457.

Hermes, C.J.L., Melo, C. & Knabben, F.T. (2010b). Algebraic solution of capillary tube flows. Part II: Capillary tube suction line heat exchangers. Appl. Therm. Eng., 30, 770–775.

Lee, W.J., Seo, J.Y., Ko, J. & Jeong, J.H. (2016). Non-equilibrium two-phase refrigerant flow at subcooled temperatures in an R600a refrigeration system. Int. J. Refrig., 70, 148–156.

Martínez-Ballester, S., Bardoulet, L., Pisano, A. & Corberán, J.M. (2017). Visualization of refrigerant flow at the capillary tube inlet of a high-efficiency household refrigerator. Int. J. Refrig., 73, 200–208.

Poling, B.E., Prausnitz, J.M., O'Connell, J.P. (2001). *The properties of gases and liquids (5th Edition)*. n.p.: McGraw-Hill.

Seixlack, A.L. & Barbazelli, M.R. (2009). Numerical analysis of refrigerant flow along non-adiabatic capillary tubes using a two-fluid model. Appl. Therm. Eng., 29, 523–531.

Yilmaz, T. & Unal, S. (1996). General equations for the design of capillary tubes. J. Fluid Eng. - T. ASME., 118, 150–154.

Zhang, C. & Ding, G. (2004). Approximate analytic solutions of adiabatic capillary tube. Int. J. Refrig., 27, 17–24.

ACKNOWLEDGMENTS

This work was carried out at the POLO Labs under the auspices of the National Institutes of Science and Technology (INCT) Program (CNPq Grant No. 404023/2019-3; FAPESC Grant No. 2019TR0846). The first author duly acknowledges the Slovenian Research Agency for supporting his sabbatical stay at POLO/UFSC through the Young Researcher program.